JEE Journal of Ecological Engineering

Journal of Ecological Engineering 2023, 24(1), 51–65
https://doi.org/10.12911/22998993/155953
ISSN 2299–8993, License CC-BY 4.0

Received: 2022.09.25
Accepted: 2022.11.09
Published: 2022.12.01

Chromium Ions Removal by Capacitive Deionization Process: Optimization of the Operating Parameters with Response Surface Methodology

Zainab M. Issa[1], Rasha H. Salman[1*]

[1] Department of Chemical Engineering, College of Engineering, University of Baghdad, Baghdad, Iraq

* Corresponding author e-mail: rasha.habeeb@coeng.uobaghdad.edu.iq

ABSTRACT

An innovative desalination method called electrosorption or capacitive deionization (CDI) has significant benefits for wastewater treatment. This process is performed by using a carbon fiber electrode as a working electrode to remove hexavalent chromium ions from an aqueous solution. The pH, NaCl concentration, and cell voltage were optimized using the Box-Behnken experimental design (BDD) in response surface methodology (RSM) to study the effects and interactions of selected variables. To attain the relationship between the process variables and chromium removal, the experimental data were subjected to an analysis of variance and fitted with a quadratic model. The optimum conditions to remove Cr(VI) ions were: pH of 2, a cell voltage of 4.3V, and NaCl concentration of 1.4 g/L. This study demonstrated that the carbon fiber electrode was very efficient in Cr(VI) ions removal and the BBD methodology was a practical and effective strategy for predicting the results of various experimental conditions during a CDI process for the removal of chromium ions.

Keywords: capacitive deionization, electrosorption, carbon fiber, chromium, wastewater.

INTRODUCTION

An increasing populace causes evolution in the development of industries to fulfil human needs. This increase has a bad influence on the environment, human health, and watery life through discharging senior quantities of wastewater that hold, non-degradable, poisonous heavy metals in the water. Subsequently, it is insistent to treat the wastewater to evacuate or bring it to allowable level concentration by different methods (KV et al., 2017; Gaikwad and Balomajumder, 2017; Chen et al., 2019). Heavy metals are an environmental issue since they are detrimental to human health even if they exist at trace levels with effectiveness extending from intense toxic effects to carcinogenic due to periodic exposure. These metals have the property of high density or atomic weight (Chen et al., 2020; Peng, Leng and Guo, 2019). Metals, in contrast to most organic contaminants, are especially hazardous since they are not biodegradable and may accumulate in biological cells, As a result, they get denser through the food chain (Barrera-Díaz et al. 2012). Chromium is a primary concern for the Environmental Protection Agency (EPA) because of its widespread use and severe toxicity. It is one of the ten most often found groundwater pollutants at the location of risky waste and one of the 14 most dangerous heavy metals, particularly when present in the hexavalent form (Su et al., 2018). In industrial, chromium compounds are utilized in electroplating, metal polishing, leather tanning, pigments, chemical manufacturing, brass, electrical, and electronic equipment (Kimbrough et al., 1999). Chromium ions depart the environment as Cr(VI) and Cr(III), and they endanger natural life and public health since they are non-biodegradable, pathogenic, and cancerous. Because of its high solubility, Cr(VI) has high mobility in water bodies and is often regarded as 500–1000 times more harmful than Cr(III). Cr(III) has a lesser solubility in water and rapidly leads to the formation of $Cr(OH)_3$ under an alkaline to an acid environment

(Liu et al., 2011; Barrera-Díaz et al., 2012). Many techniques for removing Cr(VI) have been proved to be effective, including ion exchange, electrochemical treatment, chemical precipitation, coagulation, chemical reduction, adsorption (Majeed et al., 2018, Peng et al., 2019), and CDI (Gaikwad et al., 2017). The CDI system is a recent advanced and globally attractive technology that is eco-friendly, with reduced energy consumption and operating expenses than other desalination systems, as well as a simplification in reproduction and maintenance if it compared to other traditional desalination processes (Gaikwad et al., 2017). The electrode material is the most significant component of any electrochemical system (Zhang et al., 2009). Nanoporous carbon materials are appropriate electrodes for electrosorption process, such as carbon aerogel, activated carbon, carbon fiber, ordered mesoporous carbon, carbon nanotube, and graphene (Hou and Huang, 2013;Hasan and Salman, 2021a). Carbon fiber (CF) is a promised material that has high electrical conductivity and chemical stability, as well as small and regular pore size. CF has been widely employed as an adsorbent and thoroughly researched in air purification and gas adsorption to date (Zhao et al., 2018).

Capacitive deionization (CDI) is a method that uses porous electrodes coupled with a low electrostatic field to electrosorbed ionic species from an aqueous medium (Zhang et al., 2020). When an electrical potential is supplied to electrodes in the electrosorption technique, charged ions move to the electrodes and electrostatically separated from aqueous solutions via the creation of an electrical double-layer (EDL) at the electrode/electrolyte interface. As a result, electrical potential and the creation of an electrical double layer are two vital criteria for obtaining high-performance of electrosorption capacity (Sun et al., 2018). Johnson and Newman (Johnson et al., 1970) established the first CDI model based on an electrical double layer in the 1970s. In this model, ion adsorption in the CDI is represented as a capacitive process; adsorption kinetics does not restrict the rate, and faradaic reactions are insignificant. The frequently applied Gouy-Chapman-Stern double layer theory adequately explained the interfacial characteristics and structures between (electrode) and electrolyte. The Gouy-Chapman-Stern model assumed that the double layer is separated into an 'interior' and a 'diffusion' area. The Helmholtz layer is the innermost layer, where ions are deposited directly on the electrode surface, while the Gouy–Chapman layer is a diffusion layer farther away from the surface (Jia and Zhang, 2016; Porada et al., 2013).

The electrochemical treatment of wastewater containing Cr(VI) can convert Cr(VI) to Cr(III) and subsequently remove it from wastewater without the formation of effluent or wasted adsorbent. To do this, the polarization of the working electrode has to be negative to release electrons for Cr(VI) reduction and then electrostatically attract and adsorb Cr(III) cations (Roberts et al., 2002 a; Wang et al., 2014). The possibility of removing hexavalent chromium from wastewater by electrosorption was investigated in different studies using different types of electrode materials. Golub and Oren conducted cyclic voltammetry studies with graphite felt electrode and discovered that Cr(VI) could be converted to oxidation state three Cr(III) and adsorbed on the electrode surface, most likely as colloidal $Cr(OH)_3$ (Roberts et al., 2002 b). Wang and Na studied the electrosorption performance in removing Cr(VI) from an aqueous solution using electrodes Fabricated from vertically aligned carbon nanotubes grown on stainless steel mesh. These CNT electrodes reduced 96% of the Cr(VI) in a 12 mg/L solution at a potential of -1.4 V in 115 minutes (Wang et al., 2014). Rana-Madaria et.al (Rana-Madaria et al., 2005) performed the reduction of Cr content in groundwater from 30–35 ppb to 8 ppb with a 1.2 V potential using electrosorption system using two electrodes of carbon aerogel in a batch cell of 2L in volume and under optimum conditions of pH = 2 and 0.8 A h, chromium content was reduced with 99.6 removal percentage.

In this work, Carbon fiber was utilized as the working electrode (cathode) in the electrosorption process for removing hexavalent chromium from an aqueous solution. The performance of this electrode was examined under different conditions of pH value, cell voltage, and ionic strength (NaCl concentration). These selected operating variables and the influence of interaction between them on the removal efficiency were determined and optimized by applying the response surface methodology using Box–Behnken experimental design.

EXPERIMENTAL WORK

Chemicals

All reagents were of analytical grade, including potassium dichromate ($K_2Cr_2O_7$) (with 99% of purity, alpha chemika, India), sulfate acid

(H_2SO_4) (with 98% of purity, alpha chemika, India), sodium hydroxide (NaOH) (with 98% of purity, alpha chemika, India), sodium chloride (NaCl) (with 99% of purity, HiMedia Laboratories Pvt.Ltd.), diphenylcarbazide ($C_{13}H_{14}N_4O$, Fluka Chemika, Switzerland), and HNO_3 (with a concentration of 69%, Central Drug House (P) Ltd.). All solutions were prepared with deionized water with conductivity = 5 µs/cm.

Modification of carbon fiber

Before each electrosorption process, the commercial carbon fiber utilized as a working electrode (cathode) was first cut into rectangle pieces (16.5×5 cm). Then these pieces were activated for 30 min with 5% of HNO_3 at 80 °C, then washed and kept in distilled water.

Electrosorption experiment

To examine the effect of different factors on Cr(VI) ions adsorption on modified carbon fiber electrode, the electrosorption process was studied in a small laboratory-scale CDI batch reactor of a 1L glass beaker containing 0.8L aqueous solution with 100 ppm as a constant initial chromium ions concentration. Two electrodes in the CDI system were utilized, carbon fiber as the working electrode and stainless steel plate (17×5×3 mm) as the counter electrode, the distance between the two electrodes was 1.5 cm. The beaker was placed on a hot plate magnetic stirring apparatus (Heidolph: MR Hei-standard, Germany), and the aqueous solution during the experiment was stirred with a constant stirring rate of 250 rpm to ensure ionic diffusion, and all experiments were conducted at room temperature at 25 °C ±1. The electrodes were connected to a direct-current power supply (UNI-T: UTP3315TF-L, China). The CDI experimental setup is schematically shown in Figure 1. The adjustment of pH before each experiment was set at the desired value by adding 1M of sodium hydroxide or 1M of sulfate acid, it was observed by using a pH meter instrument (HANNA instrument, pHep: HI98107).

For the measurement of Cr(VI) ions concentration, a water sample was drawn at certain time intervals of 30 min, and the amount of Cr(VI) ions that remained in the aqueous solution was measured according to the standard diphenylcarbazide method using a UV spectrophotometer (Thermo UV-Spectrophotometer, USA) at the maximum wavelength of 540 nm. Diphenylcarbazide reacts with Cr(VI) ions and produces a dark violet-colored complex in acidic conditions (Hasan et al., 2021 b). The removal efficiency of Cr(VI) ions and the equilibrium adsorption capacity q_e (mg/g) were calculated as follows (Hasan et al., 2021 a):

$$Re(\%) = \frac{(C_o - C_e)}{C_o} \times 100 \quad (1)$$

$$q_e = \frac{C_o - C_e}{m} \times V \quad (2)$$

where: C_o (mg/L) and C_e (mg/L) are the initial and equilibrium concentrations of Cr(VI) ions in the solution;
m is the total mass of the electrode (g);
V is the solution volume (L).

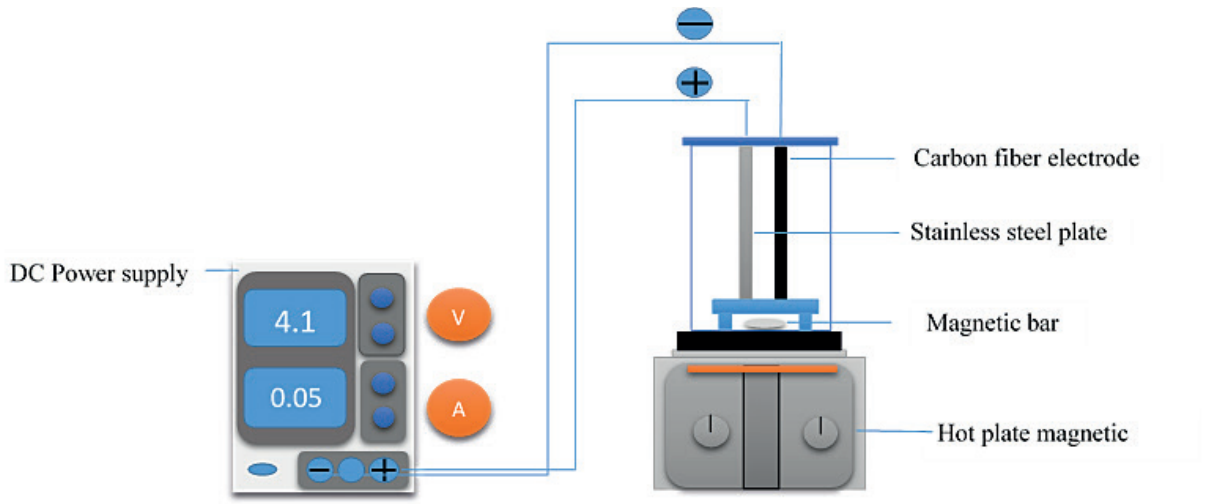

Figure 1. Schematic diagram of CDI experimental setup

Experimental design

Response surface methodology (RSM) is a Programming consisting of a set of mathematical and statistical methods that consider very useful for problem analysis and modeling in which a response of regard is affected by various variables which intend to investigate the optimum conditions to obtain the targeted response. RSM comprises an empirical modeling procedure given to the assessment of relations existing between a set of controlled experimental variables and the observed outcome (Ölmez, 2009). Subsequently, this strategy diminishes time and costs, and additionally provide more exact result from the sight of the industry. RSM leads to a fall in the number of experiments that are required to assess different parameters and their interaction (Barabadi et al., 2019).

In this work, The Box–Behnken statistical experiment design (BBD) was employed to optimize and examine the influence of selected operating variables on the removal of Cr(VI) ions from an aqueous solution using the CDI process. BBD requires moderately few combinations of variables to investigate the complex response function, and these combinations will not be all involved in which all the variables are at their highest or lowest level simultaneously. A three-factor Box–Behnken design with a three-level would give a set of experiments of 15 runs with three replicates at the central point. The number of sets of the experiment (N) developed by BBD can be calculated from:

$$N = 2k(k-1) + C_o \quad (3)$$

where: k is the number of variables and C_o is the number of central points (Kunwar P. et al., 2012). pH value (X1), NaCl concentration (X2), and cell voltage (X3) were the chosen factors and the removal efficiency (Y) of chromium ions was considered as the response. In general, each variable in Box–Behnken design consists of three levels, the three levels coded as -1, 0 and 1. The level of 1 and -1 is equal to the maximum and minimum for each input variable respectively and level 0 is equal to the middle value of the variable. Parameters were coded according to the following equation:

$$x_i = \frac{X_i - X_o}{\Delta X_i} \quad (4)$$

where: x_i is the coded value of a variable;
X_i is the real value of a variable;
X_o is the real value of a variable at the center point;
ΔX_i is the step change value (Hasan et al., 2021 a).
Process variables with their coded levels are shown in Table 1.

Box–Behnken design gives a quadratic model of a polynomial second-order equation to study the effect of the selected process variables on the obtained response, according to the following equation:

Table 1. Coded and real values of variables

Run	Blk	Coded values			Real values		
		X1	X2	X3	PH	NaCl	Voltage
1	1	0	-1	1	4	0.5	4.6
2	1	1	0	1	6	1	4.6
3	1	0	0	0	4	1	4.1
4	1	0	0	0	4	1	4.1
5	1	0	1	-1	4	1.5	3.6
6	1	1	0	-1	6	1	3.6
7	1	0	-1	-1	4	0.5	3.6
8	1	-1	0	1	2	1	4.6
9	1	0	1	1	4	1.5	4.6
10	1	0	0	0	4	1	4.1
11	1	-1	1	0	2	1.5	4.1
12	1	-1	-1	0	2	0.5	4.1
13	1	-1	0	-1	2	1	3.6
14	1	1	-1	0	6	0.5	4.1
15	1	1	1	0	6	1.5	4.1

$$Y = \beta_o + \sum_{i=1}^{k} \beta_i X_i + \\ + \sum_{i=1}^{k} \beta_{ii} X_i^2 + \sum_{i=1}^{k} \sum_{j>1}^{k} \beta_{ij} X_i X_j \quad (5)$$

where: Y represent the obtained response (removal efficiency of Cr(VI) ions);
β_o is the intercept term;
β_i is the linear term;
β_{ii} is the quadratic term;
β_{ij} is the interaction term;
X_i, X_j, …, X_k are the input variables of the process (Polat et al., 2019).
The analysis of variance (ANOVA) is also performed to investigate the significance of the selected variables and determination coefficient (R^2) is calculated to conclude the degree of model fitting.

RESULT AND DISCUSSION

The Box–Behnken model

RSM has been used to investigate the optimum condition for the selected operating variables. As mentioned previously, the most common utilized design in RSM is BBD. BBD is used to give a statistical experimental investigation of the studied process under different combinations of pH, cell voltage, and NaCl concentration to determine which variables have a significant effect on the removal efficiency of Cr(VI) ions. Table 2 shows the actual values obtained from the experimental work and the predicted values measured by RSM approaches which represent the response of the electroporation process to the removal efficiency of chromium ions. Minitab-19 software was used for experimental data analysis. By using the method of least squares (MLS) to find the best-fitting set of model variables. The least-squares approach is certainly the most often used methodology in statistics (Menke, 2015; Glaisher, 1872). The experimental data were fitted into a polynomial–second-order model to get the regression equation. The final empirical quadratic regression equation which represents the relationship between Cr(VI) ions removal efficiency and the three selected variables in terms of coded units is given in Eq. (6) as follows:

$$Y\% = -657 - 25.4\,X1 - 66.8\,X2 + \\ + 387.5\,X3 + 0.601\,X1^2 - 27.46X2^2 - 50.35X3^2 + \\ + 2.74X1 * X2 + 2.91X1 * X3 + 32.19X2 * X3 \quad (6)$$

where: Y is the removal percentage of Cr(V) ions, namely, the response; and pH (X1), NaCl concentration (X2), cell voltage (X3) are the values of the operating variables. A positive sign indicates the synergistic effects while a negative sign indicates the antagonistic effects of the factors on the respective responses.

Table 2. Experimental results of BBD for chromium ions removal

Run	Blk	pH NaCl voltage conc.			Re%	
					AC%	Pred.%
1	1	4	0.5	4.6	57.22	60.51
2	1	6	1	4.6	77.99	79.41
3	1	4	1	4.1	89.65	89.37
4	1	4	1	4.1	89.22	89.37
5	1	4	1.5	3.6	66.52	63.23
6	1	6	1	3.6	52.56	55.10
7	1	4	0.5	3.6	55.93	58.10
8	1	2	1	4.6	99.99	97.46
9	1	4	1.5	4.6	99.98	97.82
10	1	4	1	4.1	89.24	89.37
11	1	2	1.5	4.1	99.99	104.7
12	1	2	0.5	4.1	89.71	88.96
13	1	2	1	3.6	86.19	84.77
14	1	6	0.5	4.1	64.34	59.63
15	1	6	1.5	4.1	85.58	86.33

After fitting the function to the data provided by the experimental range analyzed, the analysis of variance (ANOVA) that based on the BBD was performed to check the significance and the appropriateness of the suggested polynomial quadratic models. The basic indication behind ANOVA is to give a statistical test to determine whether or not the means of numerous treatments are equal or if there is variance owing to random mistakes in the measurements of the produced responses (Singh et al., 2018). ANOVA analysis was specified based on the degree of freedom (DOF),the sum of square (SS), percentage contribution %, mean of square (MS), adjusted mean of square (Adj. MS), the adjusted sum of squares (Adj. SS), F-value, and P-value. ANOVA results are given in Table 3. As shown in Table 3, ANOVA offers the percentage contribution for each variable which represents the percentage contribution of each significant variable to the total variance that occurred in the experiment. So, the higher the percentage contribution of a variable, the more it contributes to the final results than the other variables. Any simple variation in its value will have a high effect on the response (Ahmadi et al., 2014). To explain that in detail, as can be noticed from ANOVA analysis the pH has a high contribution percentage of 29.13% compared to the contribution percentages of the cell voltage and the NaCl concentration which have a low effect on the response. The linear term has been contributed with 69.69%, while the square term and 2- way interaction term contribution percentage is 19.65% and 8.26%, respectively.

The model has a high significance which is represented by higher F-values (F model = 22.64) and lower P-values (p model = 0.001). F-value calculated from the model (F model = 22.64) is compared with the critical F value (F critical= 4.77) from the standard distribution table for the considered probability (p = 0.05) and degrees of freedom for model and error (9, 5). At this level, Fisher's F test variance ratio was sufficient to justify very high degree of adequacy of the quadratic model and the relevance of variable combinations (Kunwar P. et al., 2012). The F-value is the ratio of the model's mean square (MS) to the relevant error mean square. The higher the ratio, the higher the F-value, and the possibility that the model's variance is much higher (Garg et al., 2009). The Probability value (P-value) is utilized in the model to assess statistically significant effects. A P-value of less than 0.05 implies that the coefficients' influence is statistically significant at a 95% confidence level (Ayoubi-Feiz et al., 2014). Therefore, analysis of F-value and P-value indicated that pH and NaCl (X1 and X2) terms are the most controlling terms in the model. A significant lack of

Table 3. Analysis of variance for chromium removal

Source	DF	Seq. SS	Contribution	Adj. SS	Adj. MS	F-Value	P-Value
Model	9	3813.78	97.60%	3813.78	423.75	22.64	0.002
Linear	3	2723.13	69.69%	2723.13	907.71	48.50	0.000
PH	1	1138.07	29.13%	1138.07	1138.07	60.81	0.001
NaCl	1	900.70	23.05%	900.70	900.70	48.12	0.001
voltage	1	684.35	17.51%	684.35	684.35	36.56	0.002
Square	3	767.80	19.65%	767.80	255.93	13.67	0.008
PH*PH	1	53.71	1.37%	21.33	21.33	1.14	0.335
NaCl*NaCl	1	129.17	3.31%	174.03	174.03	9.30	0.028
voltage*voltage	1	584.92	14.97%	584.92	584.92	31.25	0.003
2-Way Interaction	3	322.85	8.26%	322.85	107.62	5.75	0.045
PH*NaCl	1	30.02	0.77%	30.02	30.02	1.60	0.261
PH*voltage	1	33.76	0.86%	33.76	33.76	1.80	0.237
NaCl*voltage	1	259.07	6.63%	259.07	259.07	13.84	0.014
Error	5	93.58	2.40%	93.58	18.72		
Lack-of-Fit	3	93.47	2.39%	93.47	31.16	534.02	0.002
Pure Error	2	0.12	0.00%	0.12	0.06		
Total	14	3907.36	100.00%				
Model summery	*S*	R^2	R^2 (adj.)	PRESS	R^2 (pred.)	AICc	BIC
	4.32626	97.60%	93.29%	1495.71	61.72%	180.03	99.82

fit suggests the model mis-adjustment. However, this result might be explained by the relatively high precision of the experimental measurements of the response variable (Kunwar P. et al., 2012). Even if a model mis-adjustment occurred, the result remains valid (Rodrigues et al., 2007).

A value of 97.60% for the coefficient of determination (R^2) indicates that predicted values agree well with the experimental data and implying that 97.60% of the variations in Cr(VI) ions removal are explained by the selected variables. The proximity of the R^2 value to 1 shows that the attained regression model is quite reliable in describing the variances in the experimental data.

Main effect plots

The main effect plot can explain the correlation between the response and the operating variable that has been selected. The main effect plot in Figure 2 depicts the effects of pH solution, cell voltage, and ionic strength on the effectiveness of Cr(VI) ion removal using the electrosorption technique.

The figure clearly shows that pH has the greatest impact on removal efficiency, as demonstrated in ANOVA analysis and the model regression equation. The effect of pH was studied in the range from 2 to 6. Experimental results show that the reduction of Cr(VI) ion increases with decreasing in pH value but a further increase in pH would decrease the reduction of Cr(VI), due to the lower amount of H^+ ion in the solution (Mohanraj et al., 2020). Because under highly acidic conditions; the presence of H^+ ions causes the cathodic reduction of Cr(VI) to Cr(III) as a proposed mechanism of hexavalent chromium reduction that presented in Eqs. 7 and 8 (Rana-Madaria et al., 2005):

$$Cr_2O_7^{2-} + 8H^+ + 6e^- \rightarrow \rightarrow Cr_2O_3 + 4H_2O \; E° = 1.33 \; V \quad (7)$$

$$HCrO_4^- + 7H^+ + 3e^- \rightarrow \rightarrow Cr^{3+} + 4H_2O \; E° = 1.35 \; V \quad (8)$$

On the other hand, the following reaction (Eq. 9) occurs at higher pH levels, and chromium may also create hydroxide in the form of $Cr(OH)_3$.

$$Cr^{3+} + 3OH \rightarrow Cr(OH)_3 \quad (9)$$

At a higher pH, this reaction occurs quickly and inhibits the reduction of Cr(VI), The pe-pH (electrode potential-pH) correlations (Pourbaix diagram) for dissolved aqueous chromium species show that chromium occurs as CrO_2^{2-}, $Cr(OH)_3$, and other hydroxyl forms at pH 4 to alkaline conditions (Rana-Madaria et al., 2005).

Both natural water and wastewater often include various ions that can alter and compete with the adsorption of other ions (Chen et al., 2015). It is clear from Figure 2 that the removal percentage increased with increasing in NaCl concentration. This increase in the number of various ions increased the system electric current, ion flow, and redox reaction but the further increase may cause inhabitation behavior which lowered or even suppressed the adsorption of chromium because of the competing forces (Huang et al., 2014).

Figure 2. Main effect plot for chromium ions removal

In Figure 2, the influence of increasing the applied voltage shows that increasing the applied voltage has a vital effect on the removal efficiency of Cr(VI) ions from the aqueous solution. This enhancement in removal efficiency in higher applied voltage conditions could be attributed to the increase in flow velocity of electrons which leads to higher raise in electrostatic attraction(Liu et al., 2011).

The response surface plot and contour plot may be used to depict the projected model equation and highlight the variance that happens when two or more parameters change at the same time. The response surface plot is a three-dimensional diagram that depicts the relationship between the response and the independent variables. The contour plot is a two-dimensional plot that corresponds to the surface plot and aids in visualizing the form of the response by drawing lines of constant response in the plane of the independent variables (Ba et al., 2007). This approach provides a better understanding of the impact of factors and their interactions on the response (Hasan et al., 2010). The RSM-BBD was used to explore the interaction effect of three variables on Cr(VI) removal efficiency, and three-dimensional and contour plots were constructed as shown in Figure 3. The hold values of the unchanged variables were fixed at their middle values (i.e. pH at 4.0, NaCl concentration at 1g/L, and voltage at 4.1V). The mutual influence on removal efficiency was investigated by changing pH from 2 to 6, NaCl concentration from 0.5 to 1.5 g/L and voltage from 3.6 to 4.6V.

As observed in the surface plot in Figure 3a, there is an obvious decrease in the removal efficiency with increasing the pH value at NaCl concentration of 0.5 g/L, whereas the decrease in the removal efficiency is lower at NaCl conc. of 1.5 g/L. Furthermore, with pH 2 the removal efficiency increased with increasing NaCl concentration to 1.5 g/L and then declined slightly as the pH reaches

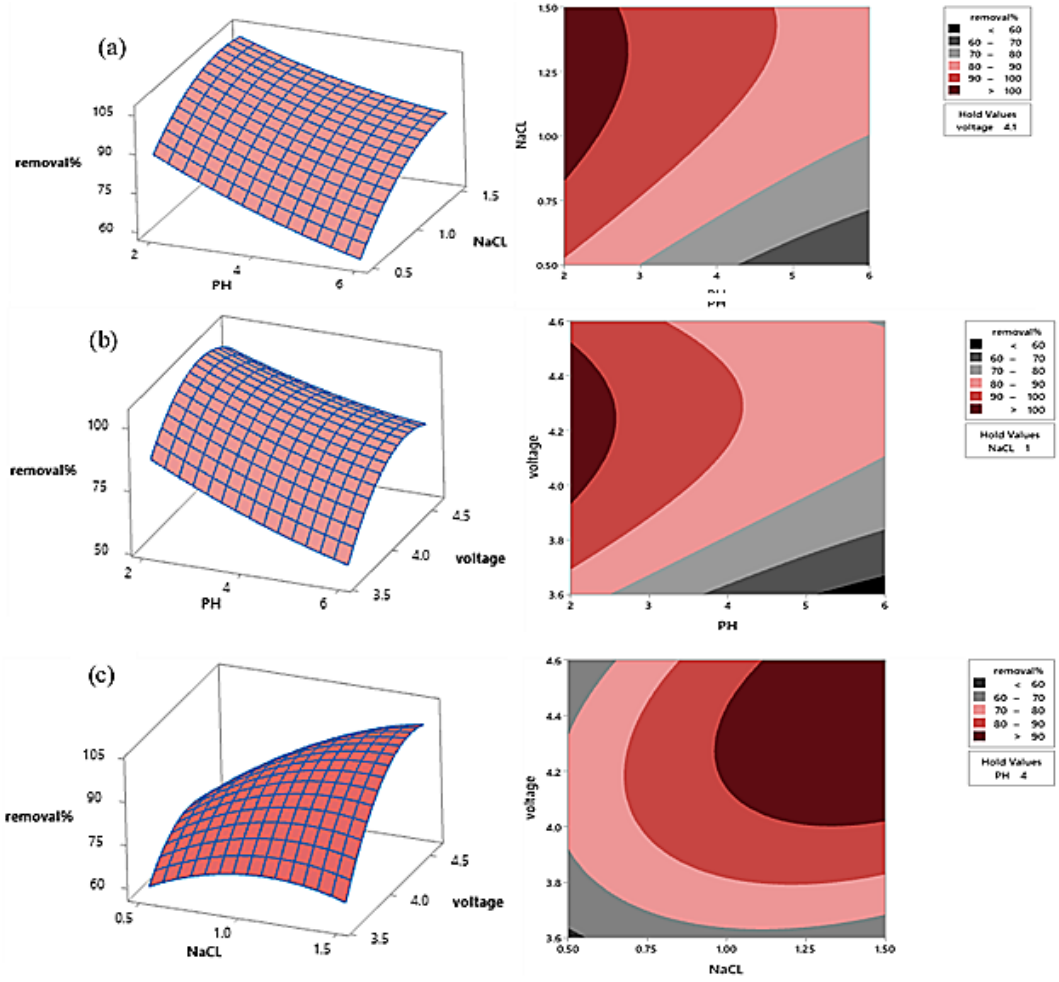

Figure 3. Response surface and contour plots for the effect of (a) solution pH and NaCl concentration (g/L), (b) solution pH and cell voltage (V) on the chromium removal (%), and (c) NaCl concentration (g/L) and cell voltage (V)

the maximum value of 6. The corresponding contour plot displays an area of dark red which represent the maximum values for removal efficiency where the pH value are ranging from 2 to 2.8 and NaCl concentration ranges from 0.8 to 1.5 g/L.

Figure 3b shows that at PH= 2, the removal efficiency increase until reaching the value of cell voltage 4.3V, and decline appear after this value, whereas the plot shows an apparent decrease in the removal efficiency with increasing the pH value at a cell voltage of 3.6V and this reduction appears to be less when cell voltage increases from 3.6 to 4.6V. It seems from the corresponding contour plot that the area of maximum values of the removal efficiency is confined between cell voltage from (3.9– 4.5V) and the PH values (2-2.5).

It appears from Figure 3c that at NaCl concentration of 1.5 g/L, the removal efficiency of Cr(VI) ions increased linearly with increasing the cell voltage from 3.6 to 4.6V, whereas there is no significant effect of cell voltage at NaCl concentration of 0.5 g/L. On the other hand, at a cell voltage of 3.6V, the removal efficiency increases very slightly until reaches the value of 1.5 g/L of NaCl concentration, while at a cell voltage of 4.6V, the removal efficiency increased with increasing NaCl concentration From 0.5 to1.5 g/L. The corresponding contour plot emphasizes that the maximum values of the removal efficiency lie in the range of cell voltage from 4-4.6V and the NaCl concentration range of 0.9– 1.5g/L.

Optimization using desirability function and conformation test

Optimization by using overall desirability was established to assess the outcomes and to achieve the best conditions for removing Cr(VI) ions from an aqueous solution. The desirability function provides information on the process's quality and acceptability (Mashile et al., 2019). This function is a mathematical approach for finding the optimal values of input parameters and output (response) simultaneously by employing the optimal input parameter levels (Islam et al., 2010). Maximum removal efficiency is achieved when the desirability function ranges from 0 to1. If the desirability value is zero, the suggested value is unfavorable. If it is 1, it means that the responsiveness has increased and the system is steady (Chockalingam et al., 2020).

To attain this goal, the three studied variables were evaluated on a specific range of values, while the analytical response was aimed to attain the maximum. The optimization results are shown in Table 4, with a desirability function of (1) for the model. Two conformation experiments were utilized under the specified optimum conditions suggested by the program. The results of these experiments are expected to be within the range obtained from the optimization analysis. Table.5 illustrates the results of the confirmation test performed on optimally selected variables. The average removal efficiency was 99.98%, and the value was very close to the suggestion.

Adsorption isotherm

Adsorption isotherms were investigated to predict the adsorption behavior and compute the adsorption capacity of carbon fiber electrode in the electrosorption process. Adsorption is typically characterized using isotherms, which are functions that link the quantity of adsorbate on the adsorbent. Several isotherm models, including Langmuir and Freundlich, can describe the

Table 4. Optimal performance of system variables for the maximum removal of chromium

Response	Goal	Lower	Target		Upper	Weight	Importance
Cr removal%	Maximum	52.569	99.99			1	1
Solution of parameters			Multiple response Prediction				
pH	NaCl	voltage	Cr removal% (Fit)	Composite desirability	SE Fit	95% CI	95% PI
2	1.43939	4.36768	108.89	1	3.70	(99.36, 118.39)	(94.24, 123.51)

Table 5. Confirmation experiments of chromium ions removal

Run	pH	NaCl concentration	Cell voltage	Re% actual	Average	AC (mg/g)
1	2	1.43939	4.36768	99.99%	99.98%	133.32
2	2	1.43939	4.36768	99.97%		133.29

distribution of metal ions between the liquid and solid phases. The Langmuir isotherm assumes monolayer coverage onto a surface with a limited number of uniform adsorption sites and no adsorbate transmigration on the surface. Once a site has filled, no more sorption may occur there. This signifies that the surface has reached a saturation point when maximal surface adsorption occurs. Langmuir models were introduced by the linearized equation as follows (Desta, 2013; Hasan et al., 2021 a):

$$\frac{Ce}{qe} = \frac{1}{b\ q_{max}} + \frac{Ce}{q_{max}} \tag{10}$$

where: qe (mg/g) is the equilibrium adsorption capacity;
Ce(mg/L) is the equilibrium concentration;
qmax (mg/g) is the maximum adsorption capacity of the adsorbent;
b is the Langmuir constant indicating the saturated capacity of adsorbents and energy term, respectively.

The Freundlich isotherm model, which describes the exponentially distribution of active sites and their energies as well as the surface heterogeneity of adsorbents, is defined by the equation below (Baseri et al., 2017):

$$qe = K_f\ Ce^{\frac{1}{2}} \tag{11}$$

where: K_f and $1/n$ are the Freundlich constants relating to adsorption capacity and intensity, respectively.

This equation can be linearized and the temperature-dependent constants K_f and $1/n$ are found by linear regression:

$$lnqe = lnK_f + \frac{1}{n} lnCe \tag{12}$$

The n value reflects the degree of nonlinearity between solution concentration and adsorption as follows: if n = 1, adsorption is linear; if n < 1, adsorption is chemical; and if n > 1, adsorption is physical. The most typical case is n > 1, which may be attributed to a dispersion of surface sites or any feature that causes a reduction in adsorbent-adsorbate contact with increasing surface density, and values of n between 1 and 10 reflect excellent adsorption (Desta, 2013).

A Batch adsorption experiment was carried out at pH 2, 4.1V, and 1g/L NaCl concentration and two different initial concentrations to determine the equilibrium time required for the carbon fiber electrode to reach its saturation point. With periodic analysis, adsorption was permitted to occur for up to 7 h, and it was discovered that adsorption for 4 hours was adequate to attain equilibrium. Figure 4 depicts the removal efficiency (Re %) vs. time (t) curve between the electrode surface and the solution.

Additional adsorption experiments were carried out to test the validity of the isotherm models by changing initial concentration of Cr(VI). The initial Cr(VI) concentrations selected were 50, 80, 100, 200, 300, 400, 500, 600 and conducted at optimal conditions. The slope and intercept of the Ce vs. qe /Ce and lnCe vs. lnqe plots, respectively, were used to compute the parameters of the Langmuir and Freundlich model equations using Minitab 19 program. The computed parameters and regression coefficient R^2 of the Langmuir and Freundlich isotherms are illustrated in Table 6 The adsorption process was found to fit well the

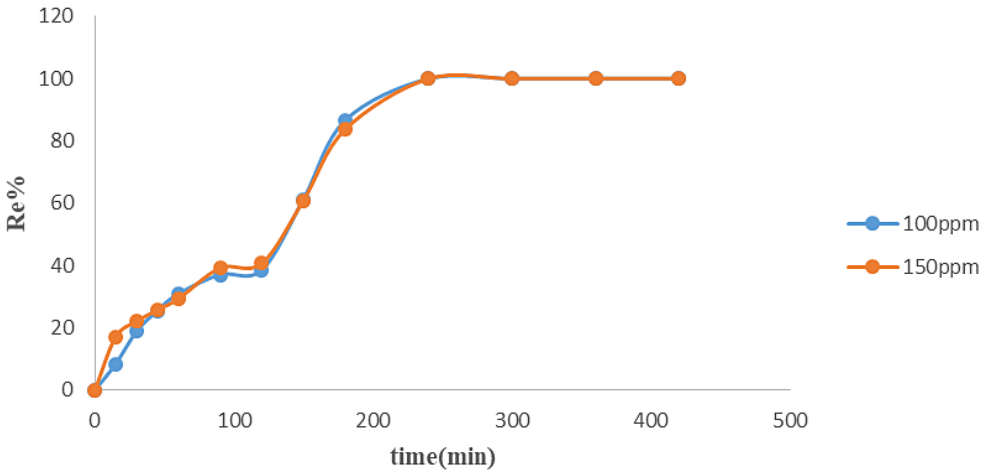

Figure 4. The removal efficiency vs. contact time between the carbon fiber electrode and the solution at conditions of pH 2, 4.1V, and 1 g/L NaCl concentration for Cr(VI) ions removal

Langmuir isotherm model than Freundlich model with maximum adsorption capacity (qmax) of 338.295 mg/g and high determination coefficient of 99.80%. For these two models, the isotherm graphical representations are presented in Figure 5.

Furthermore, the Langmuir isotherm may be expressed in terms of a separation factor (*Rl*) which is a dimensionless constant term (Avila et al., 2014, Theydan, 2018).

$$Rl = \frac{1}{1 + bC_o} \tag{13}$$

where: C_o is defined as the initial concentration (mg/L);
b is the Langmuir isotherm constant (L/mg);
Rl is the dimensionless Langmuir separation factor. The value of *Rl* was 0.966207 in the present study (As shown previously in Table 6). The range of *Rl* values is presented in Table 7 and it indicates how relevant the isotherm is. Langmuir isotherm is Favorable based on the value of *Rl* in the present study.

Table 6. Determined parameters of Langmuir and Freundlich isotherm models for chromium

Isotherm	Parameter	Value
Langmuir	qmax	338.295
	b	0.0000381
	R^2	0.9980
	Rl	0.966207
Freundlich	*Kf*(mg/g)(L/mg)$^{1/n}$	180.9101
	n	9.13242
	R^2	0.9380

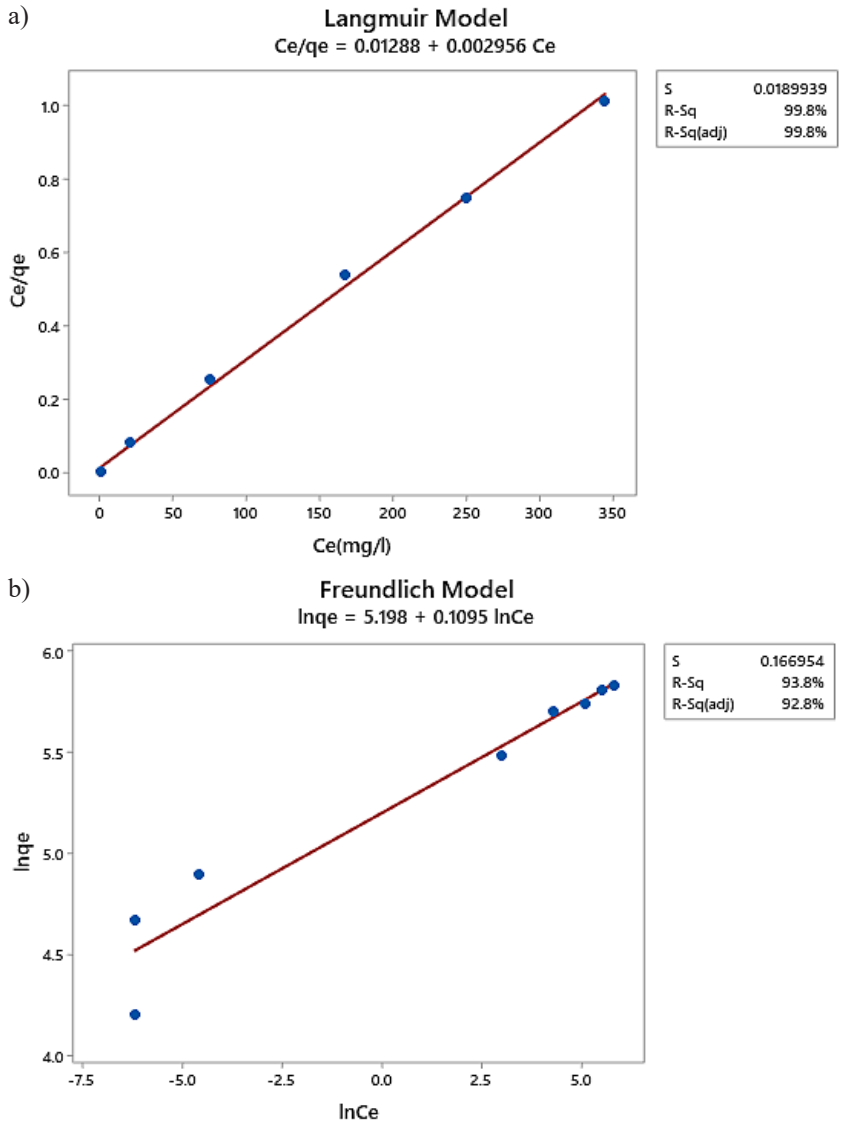

Figure 5. Adsorption isotherms of Cr(VI) ions on carbon fiber at the optimal conditions of 2 pH, 4.3 V, and 1.4 g/L NaCl concentration, the data is fitted with: (a) Langmuir model, (b) Freundlich model

Table 7. Effect of separation factor to determine the favorability of an adsorption process

Separation factor '*RI*'	Type of isotherm
RI > 1	Unfavorable
0 < *RI* < 1	Favorable
RI = 0	Irreversible
RI = 1	Linear

Table 8. Determined parameters of pseudo-first-order and pseudo second-order kinetic models for chromium ions

Kinetics	Parameter	Value
Pseudo-first-order model	qe	92.38827
	K_1	0.02701
	R^2	0.7994
Pseudo-second-order model	*Qe*	141.3827
	K_2	0.000281
	R^2	0.9918

Adsorption kinetics

One of the main features that govern the residence time of adsorbate uptake at the solid-liquid interface is the kinetics of adsorption, which describes the rate of Cr(VI) ion adsorption (Goharshadi et al., 2015). Experimental data were evaluated to identify the rate controlling mechanisms during the adsorption of Cr(VI) using two simplified kinetic models, namely pseudo-first-order, and pseudo-second-order. The pseudo-first order kinetic model is expressed by the following equation:

$$\ln(qe - qt) = lnqe - K_1 t \quad (14)$$

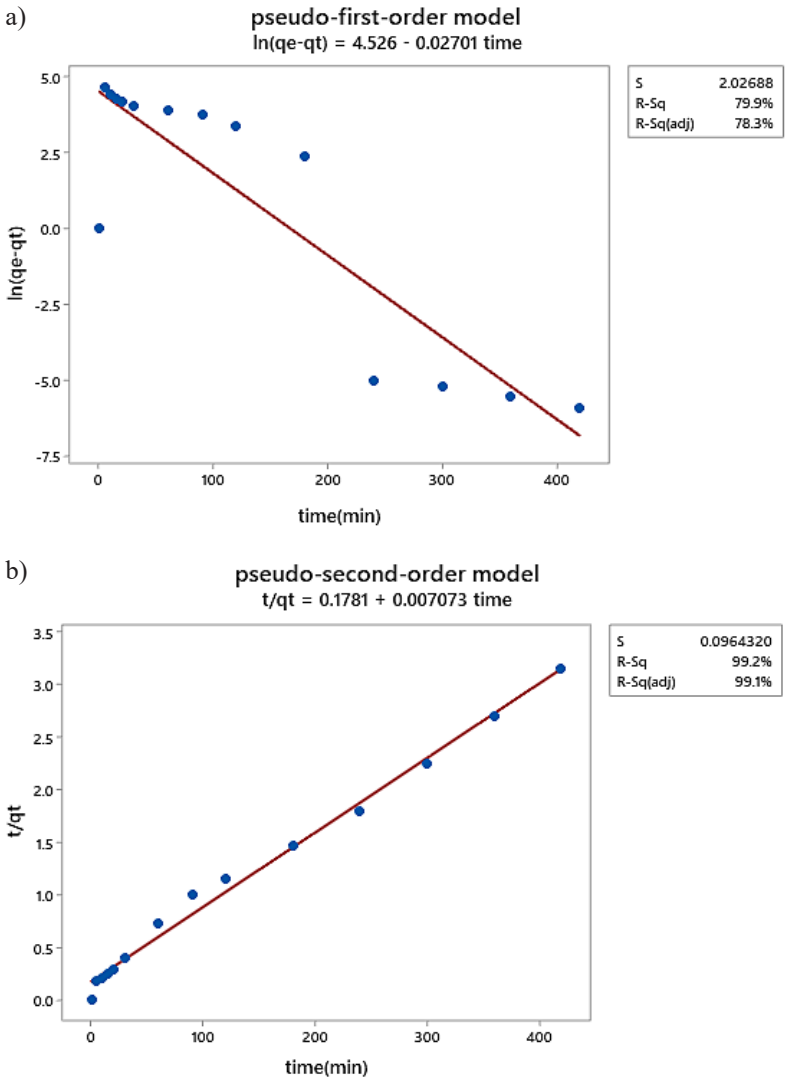

Figure 6. Kinetic graph for Cr(VI) ions removal onto carbon fiber at the optimal conditions of 2 pH, 4.3 V, and 1.4 g/L NaCl concentration with initial Cr(VI) concentration of 100 ppm, the data is fitted with: (a) pseudo-first-order model, (b) pseudo-second-order model

where: qe and qt refer to the adsorption capacity of at equilibrium and at any time, t (min), respectively;
K_1 is the rate constant of pseudo-first-order adsorption (min^{-1}).

The pseudo-second-order kinetic rate equation is expressed as follows:

$$\frac{t}{qt} = \frac{1}{K_2 qe^2} + \frac{t}{qe} \quad (15)$$

where: K_2 is the rate constant of pseudo-second order adsorption (g/mg min) (Baseri et al., 2017).
The slope and intercept of the plots of ln(qe - qt) vs.t and t/qe vs.t, respectively, were used to calculate the parameters of the pseudo-first-order and pseudo-second-order model equations using the Minitab 19 program. Table 8 illustrates the kinetics parameters and the correlation coefficient obtained from these models.

Based on the obtained correlating results of experimental data for Cr(VI) ions removal, it is clear that the determination coefficient for the pseudo-first-order model is less than 90%; this indicates that the pseudo-first-order weakly fits the experimental data. Furthermore, the determination coefficient for the pseudo-second-order model has a higher value, and the qe values calculated from the pseudo-second-order model are in good agreement with the experimental qe values than those calculated from the pseudo-first-order model. Figure 6 displays the kinetic graphical representations for the model.

CONCLUSION

A carbon fiber electrode has been used to examine its adsorption capacity in removing hexavalent Cr ions from an aqueous solution by applying an electrosorption process. The carbon fiber showed an effective removal efficiency for Cr(VI) ions in an equilibrium time of 4 h. The optimal working conditions for electrosorption Cr(VI) by the Carbon fiber electrode were: pH of 2, 4.3 V, and 1.4 g/L of NaCl concentration, which was determined using the BDD. The Cr(VI) removal percentage under optimal conditions was about 99.99%. The experimental data fitted well to the second-order polynomial model with R^2 of 0.9760. The pH has the main effect on the Cr(VI) ions removal efficiency with a contribution percentage of 29.13%. The Langmuir model was found to be the most effective model for fitting the equilibrium data. This indicates monolayer coverage on the surface of the electrode with a value of R^2 = 0.9980 and the maximum adsorption capacity was determined to be 338.295 mg/g at optimum conditions. The *Rl* value in the current study was less than one, indicating that the metal ion's successful adsorption onto carbon fiber electrode. The adsorption kinetics was well represented by the pseudo-second-order model.

REFERENCES

1. Ahmadi A., Heidarzadeh S., Mokhtari A.R., Darezereshki E., Harouni H.A. 2014. Optimization of heavy metal removal from aqueous solutions by maghemite (γ-Fe2O3) nanoparticles using response surface methodology. Journal of Geochemical Exploration., 147, 151–158.
2. Avila M., Burks T., Akhtar F., Göthelid M., Lansåker P.C., Toprak M.S., Muhammed M., Uheida A. 2014. Surface functionalized nanofibers for the removal of chromium (VI) from aqueous solutions. Chemical Engineering Journal., 245, 201–209.
3. Ayoubi-Feiz B., Aber S., Khataee A., Alipour E. 2014. Electrosorption and photocatalytic one-stage combined process using a new type of nanosized TiO2/activated charcoal plate electrode. Environmental Science and Pollution Research., 21, 8555–8564.
4. Ba D., Boyaci I.H. 2007. Modeling and optimization i: Usability of response surface methodology. Journal of Food Engineering., 78, 836–845.
5. Barabadi H., Honary S., Ebrahimi P., Alizadeh A., Naghibi F., Saravanan M. 2019. Optimization of myco-synthesized silver nanoparticles by response surface methodology employing Box-Behnken design. Inorganic and Nano-Metal Chemistry., 49, 33–43.
6. Barrera-Díaz C.E., Lugo-Lugo V., Bilyeu B. 2012. A review of chemical, electrochemical and biological methods for aqueous Cr(VI) reduction. Journal of Hazardous Materials., 223–224, 1–12.
7. Baseri H., Tizro S. 2017. Treatment of nickel ions from contaminated water by magnetite based nanocomposite adsorbents: Effects of thermodynamic and kinetic parameters and modeling with Langmuir and Freundlich isotherms. Process Safety and Environmental Protection., 109, 465–477.
8. Chen L., Wang C., Liu S., Zhu L. 2019. Investigation of adsorption/desorption behavior of Cr(VI) at the presence of inorganic and organic substance in

membrane capacitive deionization (MCDI). Journal of Environmental Sciences (China)., 78, 303–314.

9. Chen R., Sheehan T., Ng J.L., Brucks M., Su X. 2020. Capacitive deionization and electrosorption for heavy metal removal. Environmental Science: Water Research and Technology., 6, 258–282.
10. Chen Y., Peng L., Zeng Q., Yang Y., Lei M., Song H., Chai L., Gu J. 2015. Removal of trace Cd(II) from water with the manganese oxides/ACF composite electrode. Clean Technologies and Environmental Policy., 17, 49–57.
11. Chockalingam N.M.K., Kalaiselvan R.P.K. 2020. Optimization of CNC-WEDM Parameters for AA2024 / ZrB2 in situ Stir Cast Composites Using Response Surface Methodology. Arabian Journal for Science and Engineering.
12. Desta M.B. 2013. Batch sorption experiments: Langmuir and freundlich isotherm studies for the adsorption of textile metal ions onto teff straw (eragrostis tef) agricultural waste. Journal of Thermodynamics., 1.
13. Gaikwad M.S., Balomajumder C. 2017. Simultaneous electrosorptive removal of chromium(VI) and fluoride ions by capacitive deionization (CDI): Multicomponent isotherm modeling and kinetic study. Separation and Purification Technology., 186, 272–281.
14. Garg U.K., Kaur M.P., Sud D., Garg V.K. 2009. Removal of hexavalent chromium from aqueous solution by adsorption on treated sugarcane bagasse using response surface methodological approach. Desalination., 249, 475–479.
15. Glaisher J.W.L. 1872. The method of least squares [5]. Nature., 6, 329.
16. Goharshadi E.K., Moghaddam M.B. 2015. Adsorption of hexavalent chromium ions from aqueous solution by graphene nanosheets: Kinetic and thermodynamic studies. International Journal of Environmental Science and Technology, 12, 2153–2160.
17. Hasan J.T., Salman R.H., 2021a. Electrosorption of cadmium ions from the aqueous solution by a MnO2/carbon fiber composite electrode. Desalination and Water Treatment, 243, 187–199.
18. Hasan J.T., Salman R.H. 2021b. Preparation of nanostructured MnO2/carbon fiber composite electrode for removal of Cu2+ions from aqueous solution by electrosorption process. AIP Conference Proceedings, 2372.
19. Hasan S.H., Ranjan D., Talat M. 2010. of Hexavalent Chromium: Optimization of Process. BioResources, 5, 563–575.
20. Hou C.H., Huang C.Y. 2013. A comparative study of electrosorption selectivity of ions by activated carbon electrodes in capacitive deionization. Desalination, 314, 124–129.
21. Huang L., Xue J., Jin F., Zhou S., Wang M., Liu Q., Huang L. 2014. Study on mechanism and influential factors of the adsorption properties and regeneration of activated carbon fiber felt (ACFF) for Cr(VI) under electrochemical environment. Journal of the Taiwan Institute of Chemical Engineers, 45, 2986–2994.
22. Islam A., Nikoloutsou Z., Sakkas V. 2010. International Journal of Environmental Statistical optimisation by combination of response surface methodology and desirability function for removal of azo dye from aqueous solution. International Journal of Environmental Analytical Chemistry, 90, 37–41.
23. Jia B., Zhang W. 2016. Preparation and Application of Electrodes in Capacitive Deionization (CDI): a State-of-Art Review. Nanoscale Research Letters., 11, 1–25.
24. Johnson A.M., Venolia A.W., Newman J., Wilbourne R.G., Wong C.M., Gillam W.S., Johnson S., Horowitz R.H. 1970. Electrosorb Process for Desalting Water, Office of Saline Water Research and Development Progress Report No. 516, US Dept. Interior Pub., 200, 31.
25. Kimbrough D.E., Cohen Y., Winer A.M., Creelman L., Mabuni C. 1999. A critical assessment of chromium in the environment. Critical reviews in environmental science and technology., 29, 1–46.
26. Kunwar P., Singh A.K., Singh U.V., Verma P. 2012. Optimizing removal of ibuprofen from water by magnetic nanocomposite using Box-Behnken design. Environmental Science and Pollution Research., 19, 724–738.
27. Kv B., Bm N., Mnk H., Krishna R.H. 2017. An Efficient Removal of Toxic Cr(VI) from Aqueous Solution by MnO2 Coated Polyaniline Nanofibers: Kinetic and Thermodynamic Study. Journal of Environmental & Analytical Toxicology, 7.
28. Liu Y.X., Yuan D.X., Yan J.M., Li Q.L., Ouyang T. 2011. Electrochemical removal of chromium from aqueous solutions using electrodes of stainless steel nets coated with single wall carbon nanotubes. Journal of Hazardous Materials., 186, 473–480.
29. Majeed N. S.,Naji D. M., 2018. Statistical analysis of the removal of chromium(VI) by Iron Oxide Nanoparticals(Fe3O4). Journal of engineering., 24, 62–79.
30. Mashile P.P., Dimpe M.K., Nomngongo P.N. 2019. Toxic / Hazardous Substances and Environmental Engineering Application of waste tyre-based powdered activated carbon for the adsorptive removal of cylindrospermopsin toxins from environmental matrices: Optimization using response surface methodology and. Journal of Environmental Science and Health, Part A., 0, 1–7.
31. Menke W. 2015. Review of the Generalized Least Squares Method. Surveys in Geophysics., 36, 1–25.

32. Mohanraj P., Allwin Ebinesar J.S.S., Amala J., Bhuvaneshwari S. 2020. Biocomposite based electrode for effective removal of Cr (VI) heavy metal via capacitive deionization. Chemical Engineering Communications., 207, 775–789.
33. Ölmez T. 2009. The optimization of Cr(VI) reduction and removal by electrocoagulation using response surface methodology. Journal of Hazardous Materials., 162, 1371–1378.
34. Peng H., Leng Y., Guo J. 2019. Electrochemical removal of chromium (VI) from wastewater. Applied Sciences (Switzerland), 9.
35. Polat S., Sayan P. 2019. Application of response surface methodology with a Box–Behnken design for struvite precipitation. Advanced Powder Technology., 30, 2396–2407.
36. Porada S., Borchardt L., Oschatz M., Bryjak M., Atchison J.S., Keesman K.J., Kaskel S., Biesheuvel P.M., Presser V. 2013. Direct prediction of the desalination performance of porous carbon electrodes for capacitive deionization. Energy and Environmental Science., 6, 3700–3712.
37. Rana-Madaria P., Nagarajan M., Rajagopal C., Garg B.S. 2005. Removal of chromium from aqueous solutions by treatment with carbon aerogel electrodes using response surface methodology. Industrial and Engineering Chemistry Research., 44, 6549–6559.
38. Roberts E.P.L., Yu H. 2002a. Chromium removal using a porous carbon felt cathode. Journal of Applied Electrochemistry., 32, 1091–1099.
39. Roberts E.P.L., Yu H. 2002b. Chromium removal using a porous carbon felt cathode, 1091–1099.
40. Rodrigues P.M.S.M., Esteves da Silva J.C.G., Antunes M.C.G. 2007. Factorial analysis of the trihalomethanes formation in water disinfection using chlorine. Analytica Chimica Acta., 595, 266–274.
41. Singh H., Sonal S., Mishra B.K. 2018. Hexavalent chromium removal by monopolar electrodes based electrocoagulation system: optimization through Box–Behnken design. Journal of Water Supply: Research and Technology—AQUA., 67, 147–161.
42. Su X., Kushima A., Halliday C., Zhou J., Li J., Hatton T.A. 2018. Electrochemically-mediated selective capture of heavy metal chromium and arsenic oxyanions from water. Nature Communications., 9.
43. Sun Z., Chai L., Liu M., Shu Y., Li Q., Wang Y., Qiu D. 2018. Effect of the electronegativity on the electrosorption selectivity of anions during capacitive deionization. Chemosphere, 195, 282–290.
44. Theydan S. K., 2018. Effect of process variables, adsorption kinetics and equilibrium studies of hexavalent chromium removal from aqueous solution by date seeds and its activated carbon by ZnCl2. Iraqi Journal of Chemical and Petroleum Engineering., 19, 1–12.
45. Wang H., Na C. 2014. Binder-free carbon nanotube electrode for electrochemical removal of chromium. ACS Applied Materials and Interfaces, 6, 20309–20316.
46. Zhang X., Zuo K., Zhang X., Zhang C., Liang P. 2020. Selective ion separation by capacitive deionization (CDI) based technologies: A state-of-the-art review. Environmental Science: Water Research and Technology, 6, 243–257.
47. Zhang Y., Feng H., Wu X., Wang L., Zhang A., Xia T., Dong H., Li X., Zhang L. 2009. Progress of electrochemical capacitor electrode materials: A review. International Journal of Hydrogen Energy, 34, 4889–4899.
48. Zhao X., Jia B., Sun Q., Jiao G., Liu L., She D. 2018. Removal of Cr^{+6} ions from water by electrosorption on modified activated carbon fibre felt. Royal Society Open Science, 5.